Liquid Crystals
Publication details, including instructions for authors and subscription information:
http://www.informaworld.com/smpp/title~content=t713926090

Carbazole nematic liquid crystals

Weixiao Bao[a]; Muralidhar Reddy Billa[a]; Krishna Kassireddy[a]; Marta Haro[b]; Michael J. Kelly[c]; Stuart P. Kitney[a]; Manea S. Al Kalifah[b]; Pan Wei[d]; Dewen Dong[d]; Mary O'Neill[b]; Stephen M. Kelly[a]
[a] Department of Chemistry, University of Hull, Hull, UK [b] Department of Physics, University of Hull, Hull, UK [c] Department of Chemistry, University of Oxford, Oxford, UK [d] Department of Chemistry, Northeast Normal University, Changchun, China

Online publication date: 20 October 2010

To cite this Article Bao, Weixiao , Reddy Billa, Muralidhar , Kassireddy, Krishna , Haro, Marta , Kelly, Michael J. , Kitney, Stuart P. , Al Kalifah, Manea S. , Wei, Pan , Dong, Dewen , O'Neill, Mary and Kelly, Stephen M.(2010) 'Carbazole nematic liquid crystals', Liquid Crystals, 37: 10, 1289 — 1303
To link to this Article: DOI: 10.1080/02678292.2010.504862
URL: http://dx.doi.org/10.1080/02678292.2010.504862

Liquid Crystals,
Vol. 37, No. 10, October 2010, 1289–1303

Taylor & Francis
Taylor & Francis Group

Carbazole nematic liquid crystals

Weixiao Bao[a], Muralidhar Reddy Billa[a], Krishna Kassireddy[a], Marta Haro[b], Michael J. Kelly[d], Stuart P. Kitney[a], Manea S. Al Kalifah[b], Pan Wei[c], Dewen Dong[c], Mary O'Neill[b] and Stephen M. Kelly[a]*

[a]*Department of Chemistry, University of Hull, Hull, UK;* [b]*Department of Physics, University of Hull, Hull, UK;* [c]*Department of Chemistry, Northeast Normal University, Changchun, China;* [d]*Department of Chemistry, University of Oxford, Oxford, UK*

(*Received 13 March 2010; final version received 24 June 2010*)

A number of calamitic 2,7-diary-*N*-alkyl-substituted carbazoles with an enantiotropic nematic phase have been prepared. Branching of the aliphatic chain attached to the nitrogen atom in the carbazole ring leads to significantly lower liquid crystal transition temperatures. These new materials show a lower ionisation potential than fluorene analogues and blue photoluminescence in solution and as thin solid films.

Keywords: carbazoles; nematics; organic semiconductors

1. Introduction

Liquid crystals have been developed as new classes of organic semiconductor with high stability, good charge transport and/or efficient photoluminescence and electroluminescence for use in Organic Field Effect Transistors (OFETs), Organic Light-Emitting Diodes (OLEDs) and Organic Photovoltaics (OPVs) [1–8]. Liquid crystalline organic semiconductors can be deposited from solution from common organic solvents, for example by spin coating or inkjet printing, which renders them compatible with roll-to-roll large-scale manufacture of electronic components for the emerging plastic electronics industry. Polymerisable liquid crystal monomers with a polymerisable group at the end of two terminal spacer groups attached to the molecular core (reactive mesogens) are especially attractive for such applications as they can be photochemically polymerised and patterned to form an insoluble polymer network to facilitate the stepwise fabrication of multilayer devices [3–6].

A number of bisindenocarbazoles with a large fused and planar aromatic core and a methyl group attached to the bridging nitrogen atom of the carbazole moiety have been reported to exhibit a nematic phase, blue photoluminescence ($\lambda_{max} = \sim 400$ nm) with a high quantum efficiency of emission in solution ($QE_{PL} = \sim 40\%$) and stability to oxidation ($T_{degradation} > 300^{\circ}C$) (9,10). Such liquid crystalline organic semiconductors are attractive as potential charge transport layers in OFETs and OLEDs and as electron donors in OPVs. Unfortunately, the melting points of these bisindenocarbazoles are very high (Cr–N $> 180^{\circ}C$) and they do not appear to exhibit an observable glass transition on supercooling below the melting point, although some closely related, but non-liquid crystalline, bisindenocarbazoles with longer branched chains attached to the bridging nitrogen atom do exhibit high glass transiton temperatures ($74^{\circ}C$ T_g $106^{\circ}C$) despite high melting points (Cr–I $> 250^{\circ}C$) [11].

Therefore, it appeared worthwhile to synthesise a limited number of model *N*-alkyl-substituted carbazoles with a smaller, less rigid aromatic core than that of bisindenocarbazoles and with longer, more flexible, straight and branched aliphatic chains attached to the bridging nitrogen atom, and to investigate the correlation between the molecular structure of these compounds and their liquid crystalline behaviour and temperatures as well as other physical properties of relevance to plastic electronic devices. The *N*-alkyl-substituted carbazoles to be synthesised incorporate a central carbazole with different alkyl chains at the 9-position and 4-octyloxy-biphenyl-4"-yl groups in the 2,7-positions on the carbazole moiety in order to induce low melting points. It was hoped that the new *N*-alkyl-substituted carbazoles would exhibit a low melting point (Cr–N), a high glass transition temperature (T_g) and a high nematic clearing point (N–I), i.e. a nematic phase over a broad temperature range to facilitate room temperature processing and a high degree of order in the nematic phase. The most promising lead compounds, e.g. with the lowest melting point, could then be synthesised as analogues with polymerisable endgroups (reactive mesogens) with even lower melting points, due to the presence of the bulky polymerisable endgroups, so that they could then form an insoluble polymer network on polymerisation to facilitate fabrication of multilayer devices by solution processing from common organic solvents by spin coating or inkjet printing, for example. The

*Corresponding author. Email: s.m.kelly@hull.ac.uk

ISSN 0267-8292 print/ISSN 1366-5855 online

DOI: 10.1080/02678292.2010.504862
http://www.informaworld.com

presence of the *N*-alkyl-substituted carbazole moiety in the centre of the reactive mesogen should prevent oxidation at this position and induce a higher stability of these compounds, and longer lifetimes. Liquid crystalline carbazoles with columnar phases have already been reported as photoconductors with relatively high charge mobility ($\mu = 10^{-3}$ cm^3 V^{-1} s^{-1}) [12–16]. Sidechain liquid crystalline polysiloxanes with carbazole sidechains have been reported to exhibit nematic and smectic mesophases [17–21].

2. Experimental details

2.1 Instrumentation

All commercially available starting materials and reaction intermediates, reagents and solvents were obtained from Aldrich, Strem Chem. Inc., Acros or Lancaster Synthesis and were used as supplied, unless otherwise stated. Tetrahydrofuran (THF) was pre-dried with sodium wire and then distilled over sodium wire under nitrogen with benzophenone indicator, as required, and was not stored. All reactions were carried out using a dry atmosphere of nitrogen unless water was present as solvent or reagent, and the temperatures were measured externally. Mass spectra were recorded using a Gas Chromatography/ Mass Spectrometer (GC/MS)-QP5050A Schimadzu with Electron Impact (EI) at a source temperature of 200°C for compounds with relative molecular mass (RMM) $<$ 800 g mol^{-1}. Mass spectra of compounds with RMM $>$ 800 g mol^{-1} were analysed using a Bruker, reflex IV, Matrix Assisted Laser Desorption/ Ionisation (MALDI), Time of Flight (TOF) MS and a 384-well microtitre plate format with a scout target. Samples were dissolved in dichloromethane (DCM) with HABA [2-(4-hydroxyphenylazo)benzoic acid] matrix (1:10 respectively). Infrared (IR) spectra were recorded using a PerkinElmer Paragon 1000 Fourier Transform-Infrared (FT-IR) spectrometer and ^{1}H NMR spectra were recorded using a JEOL Lambda 400 spectrometer with an internal standard of tetramethylsilane (TMS). Thin layer chromatography (TLC) using aluminium-backed TLC plates coated with silica gel (60 F254 Merck) and gas liquid cromatography (GLC) using a Chromopack CP3800 gas chromatograph equipped with a 10 m CP-SIL 5CB column were used to measure the reaction progress. The purification of reaction intermediates and final products was carried out by gravity column chromatography, using silica gel (40–63 microns, 60 Å) obtained from Fluorochem. A combination of TLC, GLC and elemental analysis, using a Fisons EA 1108 CHN, was used to determine the purity of the reaction intermediates and final compounds (**13;** R = -C_8H_{17}; R = -$CH(C_8H_{17})_2$); R = -$C_2H_4CH(CH_3)C_2H_4CH{=}C(CH_3)_2$) and (**18**).

2.2 Synthesis

The *N*-alkyl-bis-2,7-[4-(octyloxy)bipheny-4'-yl]carbazoles (**13;** R = C_8H_{17}; R = $C_2H_4CH(CH_3)C_2H_4CH{=}C(CH_3)_2$); R = $CH(C_8H_{17})_2$) were synthesised as shown in reaction Scheme 1 according to modified literature procedures [22, 23]. A reaction between the Grignard reagent (**1**) and ethyl formate (**2**) yielded heptadecan-9-ol (**3**), which was converted into the corresponding tosylate (**5**) by reaction with tosyl chloride (**4**) according to a literature method [24]. Nitration of 4,4'-dibromobiphenyl (**6**) using nitric acid and ethanoic acid according to a literature method [25] gave the 2,7-dibromo-2-nitrobiphenyl (**7**). A ring-closing condensation reaction was carried out using 4,4-dibromo-2-nitrobiphenyl (**7**) and triethyl phosphite as reagent and solvent to give the 2,7-dibromo-9-*H*-carbazole (**8**) [25], which was alkylated using KOH and toluene-4-sulfonic acid 1-octylnonyl ester (**5**) according to a literature method [26] to give the 2,7-dibromo-*N*-alkyl-carbazole (**9;** R = $CH(C_8H_{17})_2$). Alkylation of the 2,7-dibromocarbazole (**8**) using a similar method using sodium hydride in place of potassium hydroxide with 1-bromooctane or 8-bromo-2,6-dimethyl-oct-2-ene (citronellyl bromide) gave the *N*-alkyl-2,7-dibromo-carbazoles (**9;** R = C_8H_{17}; R = $C_2H_4CH(CH_3)C_2H_4CH{=}C(CH_3)_2$), respectively [22, 23]. The 4-bromo-4'-octyloxybiphenyl (**11**) [27] was prepared by a Williamson ether synthesis [28] using 1-bromooctane and 4-bromo-4'-hydroxybiphenyl (**10**). The dioxaborolane ester (**12**) was synthesised by lithiation of 4-bromo-4'-octyloxybiphenyl (**11**) followed by quenching with 2-isopropoxy-4,4,5,5-tetramethyl-1,3,2-dioxaborolane [22, 23]. A palladium-catalysed Suzuki aryl-aryl cross-coupling reaction [29] between the dioxaborolane ester (**12**) and the *N*-alkyl-2,7-dibromocarbazoles (**9;** R = -C_8H_{17}; R = -$C_2H_4CH(CH_3)C_2H_4CH{=}C(CH_3)_2$; R = $CH(C_8H_{17})_2$) resulted in the *N*-alkyl-bis-2,7-[4-(octyloxy)bipheny-4'-yl]carbazoles (**13;** R = -C_8H_{17}; R = -$C_2H_4CH(CH_3)C_2H_4CH{=}C(CH_3)_2$); R = -$CH(C_8H_{17})_2$). The NMR spectra of compounds the *N*-alkyl-bis-2,7-[4-(octyloxy)bipheny-4'-yl]carbazoles (**9;** R = -C_8H_{17}; R = $C_2H_4CH(CH_3)C_2H_4CH{=}C(CH_3)_2$); R = -$CH(C_8H_{17})_2$) show unexpectedly broad and multiple peaks due to atropisomerism [30].

The *N*-octyl-2,7-bis-[5-(4-octyloxyphenyl)thiophen-2-yl]carbazole (**18**) was prepared as shown in the reaction Scheme 2 according to a modified literature method [31]. Alkylation of 4-bromophenol (**14**) using 1-bromooctane in a Williamson alkylation reaction [28] gave 1-bromo-4-octyloxybenzene (**15**), which was reacted with 2-thiopheneboronic acid in a Suzuki aryl-aryl cross-coupling reaction [31] to give 1-octyloxy-4-(thiophen-2-yl)benzene (**16**). The thiophene (**16**) was lithiated in the 2-position using *n*-BuLi in THF at −78°C and quenched using tributyl tin

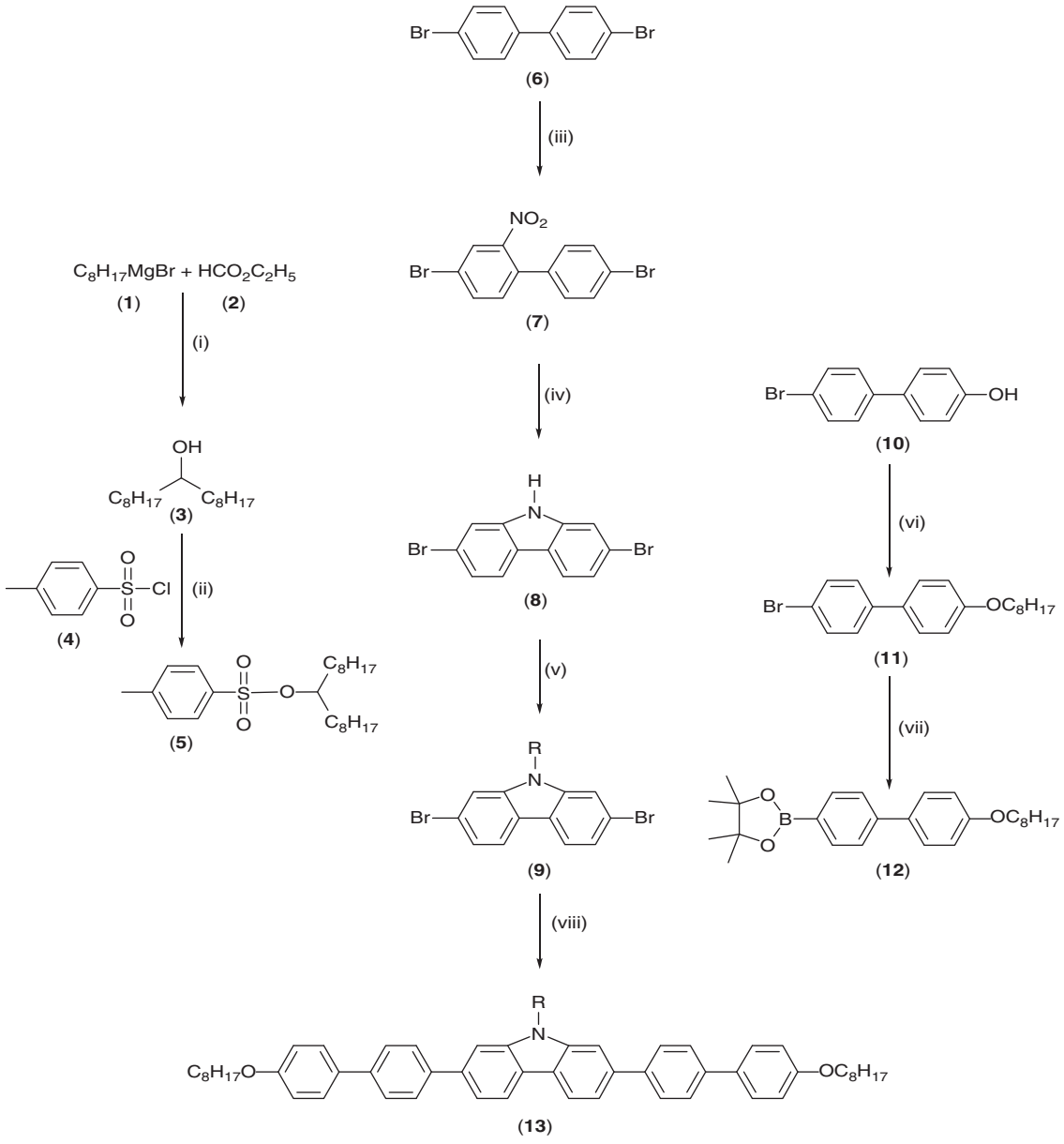

Scheme 1. Reagents: (i) THF, −78°C. (ii): $Me_3N.HCl$, TsCl, Et_3N, DCM, 0°C. (iii) HNO_3, ethanoic acid, 75°C. (iv) $P(OEt)_3$, 150°C. (v) KOH, ROTs, DMSO or NaH, RBr, DMF, 20°C. (vi) BrC_8H_{17}, K_2CO_3, butanone. (vii) (a) *n*-BuLi, THF, −78°C, (b) $C_9H_{19}BO_3$, THF, −78°C. (viii) $Pd(PPh_3)_4$, K_3PO_4, DMF, 80°C.

chloride resulting in the stannyl thiophene (**17**), which was not purified further as silica gel can protonate the 2-position of the stannyl thiophene (**17**) and remove the tin moiety [32]. A Stille aryl-aryl cross-coupling reaction [33] between 2,7-dibromo-*N*-alkyl-carbazole (**9;** R = C_8H_{17}) and the stannyl thiophene (**17**) gave the *N*-octyl-2,7-bis-{5-[4-(octyloxy)phenyl]thiophen-2-yl}carbazole (**18**).

2.2.1 *Heptadecan-9-ol* (3)

Octylmagnesium bromide (0.3000 mol, 300 cm^3 of a 1 M solution in THF) was added dropwise to a cooled, −78°C, solution of ethyl formate (**2**) (7.41 g, 0.1000 mol), in THF (167 cm^3). The mixture was allowed to warm to room temperature slowly and stirred overnight. The reaction mixture was then quenched with MeOH (100 cm^3) and the crude product extracted into DCM (4 × 50 cm^3). The combined organic layers were washed with brine (100 cm^3), dried ($MgSO_4$), filtered and concentrated under reduced pressure. The crude product was distilled under reduced pressure (b.p. 130°C at 0.5 mmHg), which yielded a white crystalline solid (20.04 g, 78%). Melting point /°C: 28–31 (Lit. 28–31 [22]). ^1H NMR ($CDCl_3$)

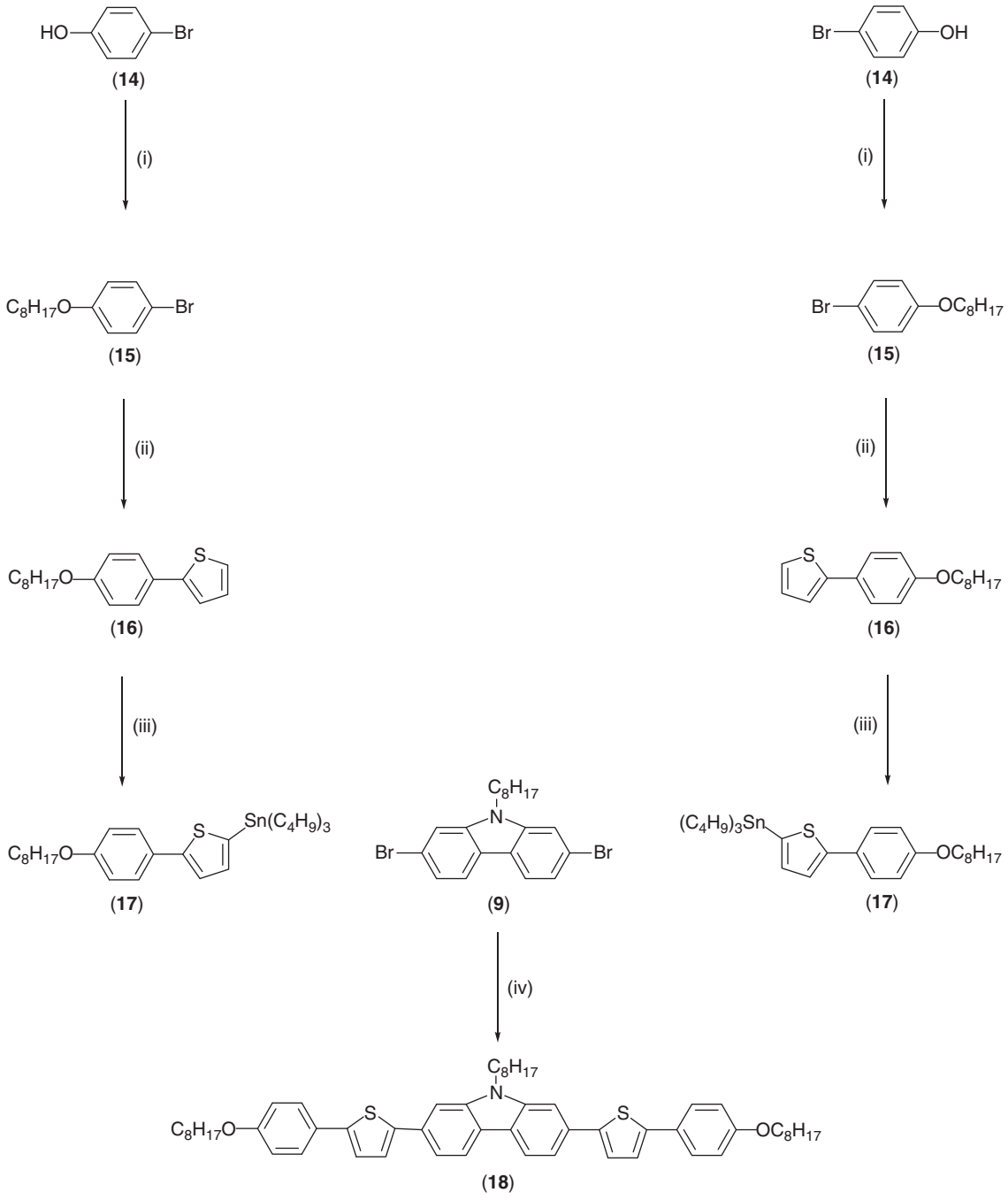

Scheme 2. Reagents: (i) $C_8H_{17}Br$, $CH_3COC_2H_5$, K_2CO_3. (ii) 2-Bromothiophene, Mg, $Pd(dppf)Cl_2$, THF. (iii) (a) *n*-BuLi, –78°C, (b) $Sn(Bu)_3Cl$, –78°C. (iv) Pd_2dba_3, PPh_3, DMF, 80°C.

δ_H: 0.87 (6H, t, $J = 7.1$ Hz), 1.28 (21H, m), 1.42 (8H, m), 3.59 (1H, m). IR ν_{max}/cm^{-1}: 3240, 2965, 2915, 2890. MS m/z (EI): 256 (M^+)

2.2.2 *Toluene-4-sulfonic acid 9-heptadecyl ester* **(5)**

4-Toluenesulfonyl chloride (**4**) (11.13 g, 0.0485 mol) in DCM (39 cm^3) was added dropwise to a cooled, 0°C, solution of heptadecan-9-ol (**3**) (10.00 g, 0.0390 mol) Et_3N (13.55 cm^3, 0.0973 mol) and $Me_3N.HCl$ (3.72 g, 0.0390 mol) in DCM (39 cm^3). The mixture was stirred for 90 min, allowed to warm to room temperature and water (100 cm^3) added. The crude product was extracted into DCM (3 × 50 cm^3) and the combined organic extracts washed with brine (100 cm^3), dried ($MgSO_4$), filtered and concentrated under reduced pressure. Purification was carried out via column chromatography [silica gel, hexane:ethyl acetate, 9:1]

to yield a colourless oil (13.75 g, 83%), which fully crystallised over 5 days. Melting point /°C: 30–32 (Lit. 31–32 [22]). ^{1}H NMR ($CDCl_3$) δ_H: 0.88 (6H, t, J = 7.1 Hz), 1.19–1.24 (24H, m), 1.53–1.55 (4H, m), 2.44 (3H, s), 4.53 (1H, quint), 7.33 (2H, d, J=8.1 Hz), 7.80 (2H, d, J = 8.2 Hz). MS m/z (EI): 411 (M^+).

2.2.3 *4,4'-Dibromo-2-nitrobiphenyl* **(7)**

A mixture of fuming HNO_3 (100%, 92.5 cm^3) and H_2O (7.5 cm^3) was added dropwise to a solution of 4,4'-dibromobiphenyl (**6**) (20.00 g, 0.0640 mol) in glacial ethanoic acid (300 cm^3) at 100°C. Once addition was complete the mixture was stirred at 100°C for 1 h, then allowed to cool to room temperature. The yellow precipitate formed was filtered and washed with copious amounts of water. The dried crude product was purified by recrystallisation from EtOH to yield a pale yellow crystalline solid (19.78 g, 87%). Melting Point /°C: 125–126 (Lit. 124, 125–127 EtOH) [25]. ^{1}H NMR ($CDCl_3$) δ_H: 8.18 (2H, dd, J = 8.83, 1.88 Hz), 8.29 (2H, d, J = 8.53 Hz), 8.38 (2H, d, J = 1.9 Hz). MS m/z (EI): 357 (M^+) Combustion analysis: Expected: C 74.95%, H 8.39%, S 11.12%. Obtained: C 74.95%, H 8.61%, S 10.97%.

2.2.4 *2,7-Dibromo-9-H-carbazole* **(8)**

A mixture of 4,4'-dibromo-2-nitrobiphenyl (**7**) (15.00 g, 0.0420 mol) and triethyl phosphite (42 cm^3, 0.1 M soln) was heated under reflux for 20 h. The excess triethyl phosphite was distilled off and the crude product purified via column chromatography [silica gel, ethyl acetate:hexane, 1:4] to yield a white crystalline solid (6.55 g, 48%). Melting point /°C: 238–239 (Lit. 236–238, 233–234 [25]). ^{1}H NMR ($CDCl_3$) δ_H: 7.35 (2H, dd, J = 8.24, 1.64 Hz), 7.57 (2H, 1.64 Hz), 7.87 (2H, d, J = 8.24 Hz), 8.13 (1H, s). MS m/z (EI): 327, 325 (M^+), 323.

2.2.5 *2,7-Dibromo-9-(heptadec-9-yl)carbazole* **(9; R = -CH(C_8H_{17})$_2$)**

A solution of toluene-4-sulfonic acid heptadec-9-yl ester (**5**) (2.78 g, 0.0068 mol) in DMSO (12.3 cm^3) was added dropwise over 1 h to mixture of 2,7-dibromo-9-*H*-carbazole (**8**) (2.00 g, 0.0062 mol), freshly powdered KOH (0.43 g, 0.0077 mol) and DMSO (12.3 cm^3) at room temperature. Upon complete addition the mixture was stirred at room temperature for 6 h then poured into water (200 cm^3) and the aqueous layer extracted with hexane (4 × 100 cm^3). The combined organic fractions were washed with brine (100 cm^3), dried ($MgSO_4$), filtered and concentrated under reduced pressure. Purification was carried out via column chromatography [silica gel, hexane:DCM, 9:1] to yield a white crystalline solid (2.89 g, 83%). Melting point /°C: 57–59 (Lit. 59–61 [22]). ^{1}H NMR ($CDCl_3$) δ_H: 0.83 (6H, t, J = 6.8 Hz), 1.13–1.26 (36 H, m), 1.90 (2H, quart), 2.20 (2H, quart), 4.41 (1H, quint), 7.32 (2H, broad m), 7.53 (1H, broad s), 7.69 (1H, broad s), 7.90 (2H, broad m). MS m/z (EI): 565, 563 (M^+), 561. Combustion analysis: Expected: C 61.82%, H 7.33%, N 2.49%. Obtained: C 62.50%, H 7.79%, N 1.85%.

2.2.6 *2,7-Dibromo-9-(octyl)carbazole* **(9; R = C_8H_{17})**

NaH (0.18 g, 60% dispersion in mineral oil, 0.0077 mol) was added in small portions to a solution of 2,7-dibromo-9-*H*-carbazole (**8**) (2.00 g, 0.0062 mol) in DMF (24.6 cm^3) and the mixture stirred for 30 min. 1-Bromooctane (1.31 g, 0.0068 mol) was added to the mixture and stirred for 18 h. The reaction was quenched with the addition of H_2O (100 cm^3) and the crude product extracted into DCM (3 × 50 cm^3). The combined extracts were washed with brine (100 cm^3), dried ($MgSO_4$), filtered and concentrated under reduced pressure. Purification was carried out via column chromatography [silica gel, DCM:hexane 3:1] to yield a white crystalline solid (2.33 g, 87%). Melting point /°C: 67–68 (Lit. 66–67 [23]). ^{1}H NMR ($CDCl_3$) δ_H: 0.87 (3H, t, J = 7.04 Hz), 1.22–1.38 (10H, m), 1.82 (2H, quint),4.20 (2H, t, J = 7.52 Hz), 7.34 (2H, dd, J = 8.28, 1.84 Hz), 7.57 (2H, 1.56 Hz), 7.89 (2H, d, J = 8.44 Hz). IR ν_{max}/cm^{-1}: 2926, 2854, 2362, 1608, 1458, 1384, 1259, 1117, 1060, 1005, 922, 816. MS m/z (EI): 439, 437 (M^+), 435.

2.2.7 *2,7-Dibromo-9-(3,7-dimethyloct-6-en-1-yl) carbazole* **(9; R = -C_2H_4CH(CH_3)C_2H_4CH=C(CH_3)$_2$)**

NaH (0.18 g, 60% dispersion in mineral oil, 0.0077 mol) was added in small portions to a solution of 2,7-dibromo-9-*H*-carbazole (**8**) (2.00 g, 0.0062 mol) in DMF (24.6 cm^3) and the mixture was stirred for 30 min. 8-Bromo-2,6-dimethyloct-2-ene (1.48 g, 0.0068 mol) was added to the mixture and stirred for 18 h. The reaction was quenched with the addition of H_2O (100 cm^3) and the crude product extracted into DCM (3 × 50 cm^3). The combined extracts were washed with brine (100 cm^3), dried ($MgSO_4$), filtered and concentrated under reduced pressure. Purification was carried out via column chromatography [silica gel, 5:1 DCM:hexane] to yield a white crystalline solid (2.41 g, 85%). Melting point /°C: 65–66. ^{1}H NMR ($CDCl_3$) δ_H: 0.85–0.88 (4H, m), 1.03 (3H, d, J = 6.56 Hz), 1.42 (1H, m), 1.99 (2H, quint), 4.19 (2H, m), 5.06 (1H, t, J = 5.6 Hz), 7.32 (2H, dd, J = 8.2, 1.6 Hz), 7.49 (2H, d, J = 1.7 Hz), 7.88 (2H, d, J = 8.4 Hz). IR ν_{max}/cm^{-1}: 3100, 3082, 3080, 2984,

2977, 2965, 2949, 2934, 2926, 2907, 1704, 1689, 1675, 1667, 1618, 1570, 1501, 1440, 1392, 1224, 1108, 1002, 581. MS m/z (EI): 465, 463 (M^+), 461.

2.2.8 *4-Bromo-4'-(octyloxy)biphenyl* (11)

A mixture of 4-bromo-4'-hydroxybiphenyl (**10**) (30.00 g, 0.1250 mol), 1-bromooctane (34.70 g, 0.1446 mol) and potassium carbonate (49.9 g, 0.3614 mol) in butanone (400 cm^3) was heated under reflux overnight. The cooled reaction mixture was filtered and the filtrate was concentrated under reduced pressure. The crude product was recrystallised from ethanol to yield a white powder (30.40 g, 70%). Melting point /°C: 120–121 (Lit. 120 [27]). Purity: >99% (GC). ^{1}H NMR ($CDCl_3$) δ_H: 0.88 (3H, t, $J = 6.7$ Hz), 1.24–1.56 (10H, m), 1.79 (2H, quint), 3.90 (2H, t, $J = 7.1$ Hz), 6.95 (2H, d, $J = 8.8$ Hz), 7.41 (2H, d, $J = 8.2$ Hz), 7.46 (2H, d, $J = 8.2$ Hz), 7.52 (2H, d, $J = 8.6$ Hz). IR ν_{max}/cm^{-1}: 3040, 2960, 2927, 2860, 1608, 1524, 1481, 1290, 1259, 1199, 1133, 1030, 814. MS m/z (EI): 362, 360 (M^+).

2.2.9 *2-[4'-(Octyloxy)biphenyl-4-yl]-4,4,5,5-tetramethyl-[1,3,2]dioxaborolane* (12)

A solution of *n*-BuLi in hexanes (13.84 cm^3, 2.5 M, 0.0346 mol) was added dropwise to a cooled (-78°C) solution of 4-bromo-4'-octyloxybiphenyl (**11**) (10.00 g, 0.0277 mol) in THF (150 cm^3). The mixture was stirred for 1 h, maintaining the temperature at −78°C, followed by the dropwise addition of 2-isopropoxy-4,4,5,5-tetramethyl-1,3,2-dioxaborolane (10.30 g, 0.0554 mol). The mixture was allowed to warm to room temperature and stirred overnight. The crude product was extracted into diethyl ether (2 × 100 cm^3), washed with water (100 cm^3), dried ($MgSO_4$), filtered and concentrated under reduced pressure. Purification was carried out via column chromatography [silica gel, DCM:hexane, 2:1] to yield a white crystalline solid (6.78 g, 60%). Melting point /°C: 89–90. ^{1}H NMR ($CDCl_3$) δ_H: 0.90 (3H, t, $J = 6.6$ Hz), 1.30–1.37 (20H, m), 1.49 (2H, quint), 1.80 (2H, quint), 4.00 (2H, t, $J = 6.1$ Hz), 6.97 (2H, d, $J = 8.8$ Hz), 7.54–7.58 (4H, m), 7.85 (2H, d, 8.9 Hz). MS m/z (EI): 408 (M^+).

2.2.10 *N-(Heptadec-9-yl)-2,7-bis[4'-(octyloxy)biphenyl-4-yl]carbazole* (13; R = -CH(C_8H_{17})$_2$)

$Pd(PPh_3)_4$ (0.10 g, 8.87×10^{-5} mol) was added to a degassed solution of 2,7-dibromo-*N*-(heptadec-9-yl)carbazole (**9; R = -CH(C_8H_{17})$_2$**) (1.00 g, 0.0018 mol) solution in DMF (3.5 cm^3), which was stirred for 10 min at room temperature. Anhydrous potassium phosphate (1.51 g, 0.0071 mol) and 2-(4'-octyloxybiphenyl-4-yl)-4,4,5,5-tetramethyl-[1,3,2]dioxaborolane (**12**) (1.75 g, 0.0044 mol) were added to the reaction mixture and the temperature increased to 80°C. The mixture was stirred overnight then allowed to cool to room temperature and water (50 cm^3) added. The crude product was extracted into DCM (3 × 50 cm^3) and the combined organic extracts washed with brine (50 cm^3), dried ($MgSO_4$), filtered and concentrated under reduced pressure. Purification was carried out via column chromatography [silica gel, 1:1 DCM:hexane] and recrystallisation from DCM/EtOH to yield a white crystalline solid (1.13 g, 66%). Transition temp./ °C: **Cr** 115 **N** 168 **I** ^{1}H NMR ($CDCl_3$) δ_H: 0.80 (6H, t, $J = 6.8$ Hz), 0.88 (6H, t, $J = 7.2$ Hz), 1.13–1.36 (40H, m), 1.44 (4H, quint), 1.80 (4H, quint), 1.99 (2H, m), 2.40 (2H, m), 4.02 (4H, t, $J = 6.4$ Hz), 4.69 (1H, broad m), 7.01 (4H, d, $J = 8.8$ Hz), 7.50 (2H, broad m), 7.61 (4H, d, $J = 8.6$ Hz), 7.69 (4H, d, $J = 8.08$ Hz), 7.76–7.79 (6H, m), 8.17 (2H, broad dd, $J = 12.48$, 8.24 Hz). IR ν_{max}/cm^{-1}: 2955, 2921, 2855, 2370, 1607, 1500, 1475, 1394, 1274, 1250, 1178, 1138, 1034, 994, 825, 810, 758, 721, 595, 518. MS m/z (MALDI): 966 (M^+). Combustion analysis: Expected: C 85.75%, H 9.49%, N 1.45%. Obtained: C 85.82%, H 9.65%, N 1.19%.

2.2.11 *2,7-bis-[4'-(Octyloxy)biphenyl-4-yl]-9-(octyl)carbazole* (13; R = C_8H_{17})

$Pd(PPh_3)_4$ (0.13 g, 1.14×10^{-4} mol) was added to a degassed solution of 2,7-dibromo-9-octylcarbazole (**9; R = C_8H_{17}**) (1.00 g, 0.0023 mol) in DMF (4.6 cm^3), which was stirred for 10 min at room temperature. Anhydrous potassium phosphate (1.95 g, 0.0091 mol) and 2-[4'-(octyloxy)biphenyl-4-yl]-4,4,5,5-tetramethyl-[1,3,2]dioxaborolane (**12**) (2.34 g, 0.0057 mol) were added to the reaction mixture and the temperature increased to 80°C. The mixture was stirred overnight then allowed to cool to room temperature and water (50 cm^3) added. The crude product was extracted into DCM (3 × 50 cm^3) and the combined organic extracts washed with brine (50 cm^3), dried ($MgSO_4$), filtered and concentrated under reduced pressure. Purification was carried out via column chromatography [silica gel, DCM:hexane, 1:1] and recrystallisation from DCM/EtOH to yield a white crystalline solid (1.16 g, 60%). Transition Temp./ °C: **Cr** 229 **N** 309 **I** ^{1}H NMR ($CDCl_3$) δ_H: 0.85 (3H, t, $J = 7.0$ Hz), 0.90 (6H, t, $J = 6.4$ Hz), 1.24–1.31 (26H, m), 1.49 (4H, quint), 1.82 (4H, quint), 1.95 (2H, quint), 4.02 (4H, t, $J = 6.6$ Hz), 4.42 (2H, t, $J = 7.3$ Hz), 7.02 (4H, d, $J = 8.9$ Hz), 7.53 (4H, dd, $J = 8.04$, 1.48 Hz), 7.61 (4H, d, $J = 8.8$ Hz), 7.63 (2H, d, $J = 1.42$ Hz), 7.69 (4H, d, $J = 8.44$ Hz), 7.79 (4H, d, $J = 8.44$ Hz), 8.16 (2H, d, $J = 8.04$ Hz). IR ν_{max}/cm^{-1}: 2925, 2854, 1600, 1489, 1466, 1422, 1385, 1342, 1288, 1093, 821, 700. MS m/z (MALDI): 839 (M^+).

Combustion analysis: Expected: C 85.77%, H 8.76%, N 1.67%. Obtained: C 85.21%, H 7.97%, N 2.01%.

2.2.12 *9-(3,7-Dimethyl-oct-6-enyl)-2,7-bis-[4'-(octyloxy)biphenyl-4-yl]carbazole* **(13; R = -$C_2H_4CH(CH_3)C_2H_4CH{=}C(CH_3)_2$)**

$Pd(PPh_3)_4$ was added to a degassed solution of 2,7-dibromo-9-(3,7-dimethyl-oct-6-enyl)carbazole (**9; R = -$C_2H_4CH(CH_3)C_2H_4CH{=}C(CH_3)_2$**) (1.00 g, 0.0022 mol) in DMF (4.3 cm^3), which was stirred for 10 min at room temperature. Anhydrous potassium phosphate (1.84 g, 0.008 mol) and 2-[4'-(octyloxy)biphenyl-4-yl]-4,4,5,5-tetramethyl-[1,3,2]dioxaborolane (**12**) (2.20 g, 0.0054 mol) were added to the reaction mixture, the temperature increased to 80°C and the resultant reaction mixture heated at this temperature overnight. The reaction mixture was allowed to cool to room temperature, water (50 cm^3) was added and the crude reaction product extracted into DCM (3 × 50 cm^3). The combined organic extracts were washed with brine (50 cm^3), dried ($MgSO_4$), filtered and concentrated under reduced pressure. Purification was carried out via column chromatography [silica gel, DCM:hexane, 1:1] and recrystallisation from DCM/EtOH to yield a white crystalline solid (0.73 g, 39%). Melting point /°C: 224 ^{1}H NMR ($CDCl_3$) δ_H: 0.90 (6H, t, $J = 7.21$ Hz), 1.09 (3H, d, $J =$ 6.2 Hz), 1.29–1.37 (20H, m), 1.49–1.51 (4H, m), 1.64 (6H, s), 1.79–1.86 (5H, m), 1.95 (2H, quint), 4.02 (4H, t, $J =$ 6.8 Hz), 4.43 (2H, m), 5.07 (1H, t, $J = 5.7$ Hz), 7.01 (4H, d, $J = 9.2$ Hz), 7.51 (2H, dd, J=8.2, 1.7 Hz), 7.59–7.62 (6H, m), 7.69 (4H, d, $J = 8.2$ Hz), 7.79 (4H, d, $J = 8.2$ Hz), 8.16 (2H, d, $J = 8.4$ Hz). IR ν_{max}/cm^{-1}: 2925, 2855, 2362, 1606, 1498, 1465, 1384, 1288, 1248, 1202, 1178, 1047, 915, 816. MS m/z (MALDI): 866 (M^+). Combustion analysis: Expected: C 85.96%, H 8.73%, N 1.62%. Obtained: C 86.71%, H 8.49%, N 2.01%.

2.2.13 *1-Bromo-4-(octyloxy)benzene* **(15)**

A mixture of 4-bromophenol (**14**) (20.00 g, 0.1156 mol), potassium carbonate (23.97 g, 0.1734 mol), 1-bromooctane (26.70 g, 0.1382 mol) and butanone (200 cm^3) was heated under reflux overnight. The cooled reaction mixture was poured into water (200 cm^3) and the crude product extracted into ethyl acetate (4 × 100 cm^3). The combined organic extracts were washed with brine (200 cm^3), dried ($MgSO_4$), filtered and concentrated under reduced pressure. Purification was carried out via column chromatography [silica gel, hexane] to yield a colourless liquid (26.12 g, 79%). Purity: >98% (GC). ^{1}H NMR ($CDCl_3$) δ_H: 0.88 (3H, t), 1.27–1.46 (12H, m), 3.90 (2H, t), 6.90 (2H, d, $J = 8.8$ Hz), 7.52 (2H, d, J=8.9 Hz). IR ν_{max}/cm^{-1}: 3040, 2960, 2927, 2860, 1608, 1524, 1481, 1290, 1259, 1199, 1133, 1030, 814. MS m/z (EI): 286, 284 (M^+). Combustion analysis: Expected: C 58.95%, H 7.42% Obtained: C 59.09%, H 7.69%.

2.2.14 *2-[4-(Octyloxy)phenyl]thiophene* **(16)**

A solution of 2-bromothiophene (17.13 g, 0.1510 mol) in THF (100 cm^3) was slowly added to a mixture of magnesium turnings (2.76 g, 0.1135 mol) and THF (50 cm^3). Once added the mixture was slowly brought to reflux and heated under reflux for a further 1 h until no more magnesium turnings were present. The Grignard reagent prepared in situ was transferred dropwise to a mixture of 1-bromo-4-(octyloxy)benzene (**15**) (25 g, 0.0876 mol), $Pd(dppf)Cl_2$ (0.25 g, 3.33 × 10^{-4} mol) and THF (50 cm^3). The resultant mixture was heated for 2 h, allowed to cool and then poured into water (150 cm^3). The crude product was extracted into DCM (3 × 200 cm^3). The combined organic extracts were washed with brine (2 × 100 cm^3), dried ($MgSO_4$), filtered and concentrated under reduced pressure. Purification was carried out via column chromatography [silica gel, DCM: hexane 1: 1] and recrystallisation from ethanol to yield a white crystalline solid (21.50 g, 80.3%). Melting point /°C: 69–72 (Lit. 68–70, EtOH [31]). ^{1}H NMR ($CDCl_3$) δ_H: 0.89 (3H, t), 1.23–1.36 (8H, m), 1.43–1.48 (2H, m), 1.79 (2H, quint), 3.98 (2H, t), 6.88 (2H, d, $J =$ 8.8 Hz), 7.04 (1H, dd, $J = 5$, 3.6 Hz), 7.19–7.21 (2H, m), 7.53 (2H, d, $J = 8.8$ Hz). IR ν_{max}/cm^{-1}: 2923, 1606, 1572, 1531, 1501, 1435, 1393, 1270, 1251, 1169, 1086, 1026, 814, 681, 537, 487. MS m/z (EI): 288 (M^+), 250, 191, 176 (M 100), 147, 115, 69, 41. 149, 131, 115, 84. Combustion analysis: Expected: C 74.95%, H 8.39%, S 11.12%. Obtained: C 74.95%, H 8.61%, S 10.97%.

2.2.15 *Tributyl{5-[4-(octyloxy)phenyl]thiophene-2-yl}stannane* **(17)**

A solution of *n*-BuLi in hexane (16.64 cm^3, 2.5 M, 0.0416 mol) was added dropwise to a cooled (-78°C) solution of 2-[4-(octyloxy)phenyl]thiophene (**16**) (10.00 g, 0.0347 mol) in THF (150 cm^3). The mixture was stirred for 1 h, maintaining the temperature at –78°C, followed by the dropwise addition of tributyl tin chloride (13.54 g, 0.0416 mol). The mixture was allowed to warm to room temperature and stirred overnight. The crude product was extracted into diethyl ether (2 × 100 cm^3), washed with water (100 cm^3), dried ($MgSO_4$), filtered and concentrated under reduced pressure. No further purification was carried out. MS m/z (EI): 576 (M^+), 575. Purity: 79%. ^{1}H NMR ($CDCl_3$) δ_H: 0.86–0.94 (12H, m), 1.12 (6H, t), 1.26–1.48 (16H m), 1.58–1.70 (8H, m), 4.00 (2H, t), 6.89 (2H, d, J = 9.0 Hz), 7.13 (1H, d, $J = 3.4$ Hz), 7.40 (1H, d, $J =$ 3.4 Hz), 7.54 (2H, d $J = 9.0$ Hz). IR ν_{max}/cm^{-1}: 3100, 3054, 2951, 2922, 2854, 1599, 1569, 1500, 1476, 1279,

1252, 1181, 1117, 1025, 930, 850, 811. MS m/z (EI): 578 (M^+), 521, (M100), 519, 465, 463, 407, 176, 145, 115, 57.

2.2.16 N-Octyl-2,7-bis-{5-[4-(octyloxy)phenyl]thiophen-2-yl}carbazole **(18)**.

A mixture of 2,7-dibromo-*N*-(octyl)carbazole (**9**) (0.4 g, 0.00092 mol) and tributyl{5-[4-(octyloxy)phenyl]thiophene-2-yl}stannane (**17**) (2.66 g, 0.0056 mol) was dissolved in DMF, tris(dibenzylideneacetone)dipalladium (0.02 g, 2.18×10^{-5}) and triphenyl phosphine (0.01 g, 4.5×10^{-5}) were added and the resultant mixture was heated at 45°C overnight. The reaction mixture was allowed to cool, poured into water (300 cm^3) and the crude product extracted into ethyl acetate (3×200 cm^3). The combined organic extracts were washed with brine (2×200 cm^3), dried $MgSO_4$ and the solvent was removed under reduced pressure. Purification was carried out via column chromatography [silica gel, 10–40% of DCM:hexane] and recrystallisation from DCM/ethanol to yield a pale yellow solid (0.42 g, 51.3%). Melting point /°C: **Cr** 163 **N** 228 **I**. ^{1}H NMR ($CDCl_3$) δ_H: 0.85–0.89 (12H, m), 1.27–1.38 (27H, m), 1.8 (4H, quint), 1.92 (2H, t), 3.99 (4H, t), 4.33 (2H, t), 6.91 (4H, d, $J = 7$ Hz), 7.20 (2H, 3.76 Hz), 7.35 (2H, 3.76 Hz), 7.52 (2H, d, $J = 6.56$ Hz), 7.59–7.62 (6H, m), 8.13 (2H, d). IR ν_{max}/cm^{-1}: 2850, 1717, 1653, 1599, 1569, 1541, 1510, 1497, 1463, 1391, 1329, 1308, 1282, 1249, 1176, 1111, 1027, 828, 815, 791, 722, 661, 633, 608. MS m/z (EI): 853, 852(M^+ M100), 815, 609, 574, 523, 507, 287. Combustion analysis: Expected: C 78.92%, H 8.16%, S 1.64%. Obtained: C 77.19%, H 7.67%, S 1.62%.

2.3 Mesomorphic properties

The mesomorphic behaviour of the compounds (**13;** R = -C_8H_{17}; -$CH(C_8H_{17})_2$); and -$C_2H_4CH(CH_3)C_2H_4CH{=}C(CH_3)_2$) and (**18**) was investigated between crossed polarisers using optical microscopy, using a Linkam 350 hot-stage and control unit in conjunction with a Nikon E400 polarising microscope. The only liquid crystalline phase observed was the nematic phase despite substantial supercooling below the melting point. Nematic droplets were observed on cooling from the isotropic liquid to form the Schlieren texture with two and four-point brushes typical of the nematic phase along with some optically extinct homeotropic areas (see Figure 1).

The nematic texture sometimes formed more optically extinct homeotropic areas as the sample was cooled further, which indicates that the phase is optically uniaxial. Both the birefringent and homeotropic areas flash brightly on mechanical disturbance. This optical behaviour, and the simultaneous presence of both the homeotropic and the Schlieren texture,

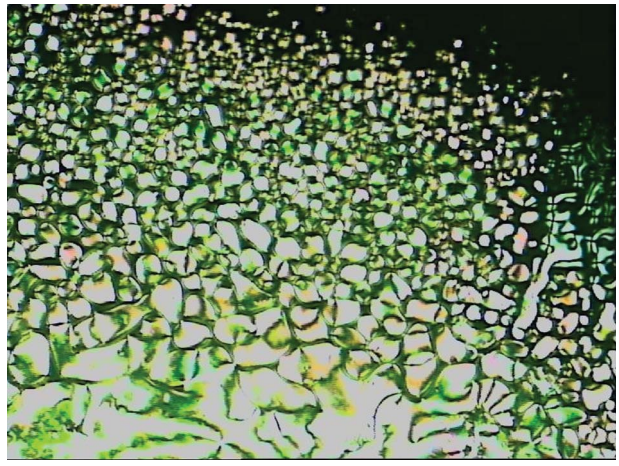

Figure 1. Part Schlieren texture part nematic droplets of the nematic phase of compound (**18**) on cooling to 225°C (colour version online).

confirms that the mesophase observed is indeed a nematic phase. The values for the liquid crystal transition temperatures of the compounds (**13;** R = -C_8H_{17}; R = -$CH(C_8H_{17})_2$); R = -$C_2H_4CH(CH_3)C_2H_4CH{=}C(CH_3)_2$) and (**18**) were confirmed by differential scanning calorimetry (DSC) using a PerkinElmer DSC-7 and in conjunction with a TAC 7/3 instrument controller, using the peak measurement for the reported value of the transition temperatures. Good agreement (≈ 1–2°C) with those values determined by optical microscopy were obtained; see Figure 2 for a characteristic DSC trace for compound (**13;** R = $CH(C_8H_{17})_2$).

These values were determined twice on heating and cooling cycles on the same sample. The values obtained for various samples of the same compounds were reproducible, and no thermal degradation was observed even at relatively high temperatures. The base line of the DSC traces is relatively flat, and sharp transition peaks were observed in each case. The melting point (Cr–N and Cr–I) and the clearing point (N–I) are both first order as expected. A degree of supercooling below the melting point was observed on the cooling cycle (e.g. see Figure 2) but no other transitions attributable to liquid crystalline phases could be observed. The enthalpy of transition between the nematic phase and the isotropic phase is relatively small for each of the compounds measured (Table 1). The enthalpy of fusion, in comparison, is at least an order of magnitude higher than that of the transition from the nematic state into the isotropic state (see Table 1) as expected, due to the much higher degree of order in the solid state than either in the nematic or the isotropic phases. Thermal gravimetric analysis (TGA) of the carbazole (**18**) and the reference 9,9-dialkyl fluorenes (**19**) was performed on a Netzsch

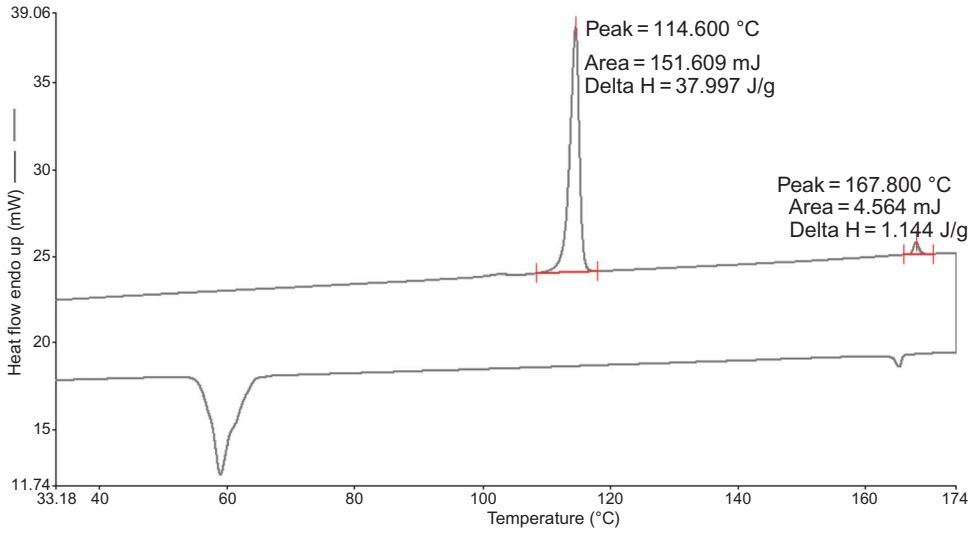

Figure 2. Differential scanning thermogram as a function of temperature for the first heating and cooling cycle for compound (**13**; R = $CH(C_8H_{17})_2$) at a scan rate of 10°C min^{-1}.

TGA TG209 thermobalance, interfaced with a Balzers ThermoStar GSD 300T mass spectrometer.

Molecular modelling was carried out using ChemDraw pro 3D MOPAC 2000, CambridgeSoft, USA, and MM1 minimisation. The chemical bonds in the compounds shown in Figures 3–5 define the molecular geometry of the aromatic core of the molecules (**18**, **13**; R = C_8H_{17}; R = $C_2H_4CH(CH_3)C_2H_4CH=C(CH_3)_2$) and **13**; R = $CH(C_8H_{17})_2$) and no assumptions about their conformation needed to be made. The disposition of the phenyl and thiophene rings of compound (**18**) shown in Figure 3 was chosen to give rise to the most linear structure in the modelling, which was based upon the assumption that the preferred molecular conformation will be that giving rise to the highest length-to-breadth (aspect) ratio and greatest degree of molecular polarisability, consistent with current understanding of the nematic phase of thermotropic calamitic liquid crystals. The preferred conformation of the aliphatic chains in the lateral and terminal positions in the compounds (**18**, **13;** R = C_8H_{17}; R = $C_2H_4CH(CH_3)C_2H_4CH=C(CH_3)_2$) and **13**; R = $CH(C_8H_{17})_2$), shown in Figures 3–5, was assumed in each case to be the all-*trans*, antiperiplanar conformation for the same reason cited above.

2.4 *Physical measurements*

The photoluminescence (PL) and optical quantum efficiency (μ) measurements were carried out with the samples inside a barium sulphate-coated integrating sphere filled with nitrogen gas [34]. A GaN laser diode with an emission wavelength of 406 nm was used as an excitation source for the sample, which was detected by an Ocean Optics S2000 photodiode array. Thin films of the liquid crystals were prepared by spin coating from a 1.5 wt% solution in toluene onto quartz substrates in a nitrogen-filled glove box. The liquid crystalline samples were subsequently baked at 120°C for 10 min and then cooled to room temperature to form the nematic phase or a glassy nematic state.

The ionisation potential (IP) of the compounds were measured electrochemically by cyclic voltammetry using a computer-controlled scanning potentiostat (Solartron 1285), which functions as wave generator, potentiostat and current-to-voltage converter. The Corrware and Corrview software packages were used to control and record the cyclic voltammetry experiments, respectively. 1 mM of the compound was dissolved in 5 cm^{-3} of an electrolytic solution of 0.3 M tetrabutylammonium hexafluorophosphate ($TBAHFP_6$) in DCM. The solution was placed in a standard three-electrode electrochemical cell. A glassy carbon electrode was used as the working electrode. Silver/silver chloride (3 M NaCl and saturated Ag/Cl) and a platinum wire were used as the reference and counter electrodes, respectively. The electrolyte was recrystallised twice before use. Oxygen contamination was avoided by purging the solution with dry argon before each measurement. The measured potentials were corrected to an internal ferrocene reference added at the end of each measurement. A typical scan rate of 20 mV s^{-1} was used, and two scans were performed to check the repeatability. A typical cyclic voltammetry scan is shown in Section 3. The onset potential for oxidation, E_{ox} is clearly defined by a step change in current and is obtained from the intersection

Table 1. Liquid crystal transition temperatures (°C) and some enthalpies of transition (J g^{-1}) for the compounds (**13**; R = -C_8H_{17}, -$C_2H_4CH(CH_3)C_2H_4CH{=}C(CH_3)_2$ and -$CH(C_8H_{17})_2$), (**18**), (**19**) and (**20**).

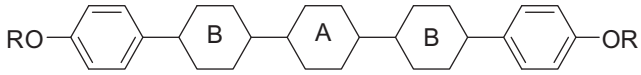

	A	B	RO	T_g	Cr	N	I
(**13**)	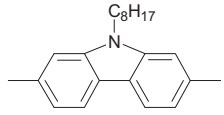	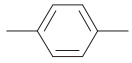	$C_8H_{19}O$	-	•	229 (53.46) •	309 (1.23) •
(**13**)	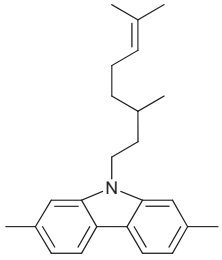	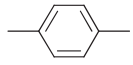	$C_8H_{19}O$	-	•	224	- •
(**13**)	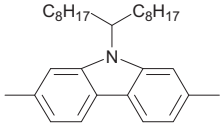	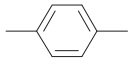	$C_8H_{19}O$	-	•	115 (38.18) •	168 (1.23) •
(**18**)	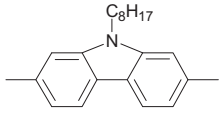	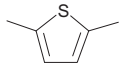	$C_8H_{19}O$	-	•	163 (34.32) •	228 (0.99) •
(**19**)	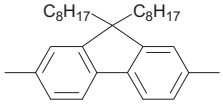	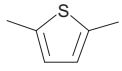	$C_8H_{19}O$	•	-12 •	69 •	99 •
(**20**)	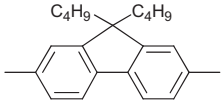	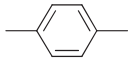	$(H_2C{=}CH)_2CHO_2CC_5H_{10}O$	•	20 •	130 •	155 •

of the two tangents at the current discontinuity based on the empirical relationship proposed by Bredas, IP = [E_{ox} + 4.4] eV [35]. We were unable to measure a value for the reduction potential because of the limited working range of the electrolyte. However, the electron affinity (EA) was estimated by subtraction of the optical band edge (E_g), taken as the energy of the onset of absorption of the compound from the IP. Although this approximation does not include a correction for the exciton binding energy, the values obtained agree within ± 0.05 eV with those measured electrochemically in our laboratory for other classes of reactive mesogen. A UV/Vis spectrometer (Lambda 40, PerkinElmer) was used to measure the optical absorption spectrum in the range 200–800 nm, for the optical energy gap, E_g, measurement. The sample material was deposited by spin coating onto a transparent or nearly transparent substrate (quartz) as a thin solid film.

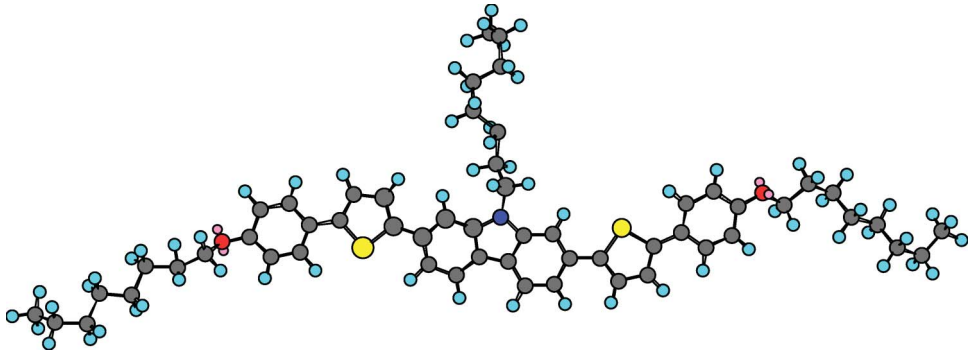

Figure 3. MM2 optimised geometry of compound (**18**) (colour version online).

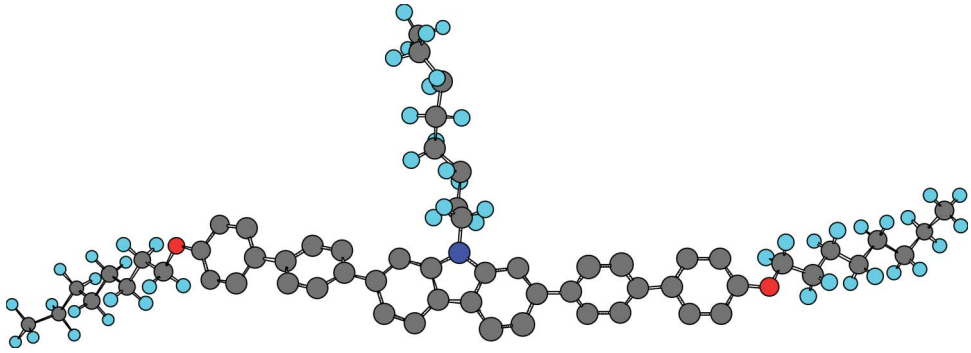

Figure 4. MM2 optimised geometry of the compound (**13**; R = C_8H_{17}) (colour version online).

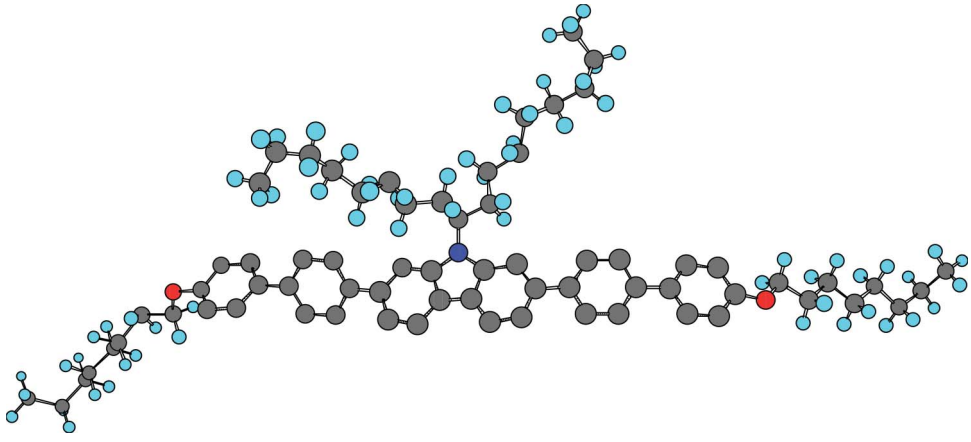

Figure 5. MM2 optimised geometry of the compound (**13**; R = $CH(C_8H_{17})_2$) (colour version online).

3. Results and discussion

3.1 Transition temperatures

The liquid crystal transition temperatures of the *N*-alkyl-2,7-bis[4'-(octyloxy)biphenyl-4-yl]carbazoles (**13;** R = -C_8H_{17}; R = -$CH(C_8H_{17})_2$); R = -$C_2H_4CH(CH_3)C_2H_4CH{=}C(CH_3)_2$), *N*-octyl-2,7-*bis*-{5-[4-(octyloxy)phenyl]thiophen-2-yl}carbazole (**18**) and the analogous 9,9-dioctyl-substituted fluorene (**19**) are collated in Table 1. A nematic phase was observed for all compounds, and no smectic phases were identified despite substantial cooling below the melting point. The melting point of these carbazoles is significantly above room temperature, but also lower than those of related bisindenocarbazoles [9, 10]. The *N*-octyl-2,7-bis[4'-(octyloxy)biphenyl-4-yl]carbazole (**13**; R = -C_8H_{17}) forms an enantiotropic nematic mesophase (309°C) above a very high melting point (229°C). The corresponding *N*-octyl-2,7-*bis*-{5-[4-

(octyloxy)phenyl]thiophen-2-yl}carbazole (**18**) with two thiophene rings next to the carbazole unit in place of two phenyl rings also exhibits an enantiotropic nematic phase. However, the *N*-octyl-2,7-*bis*-{5-[4-(octyloxy)phenyl]thiophen-2-yl}carbazole (**18**) exhibits a significantly lower melting point (163°C) and a much lower nematic clearing point (228°C) as well as a narrower nematic phase compared with the values observed for the *N*-octyl-2,7-bis[4'-(octyloxy)-biphenyl-4-yl]carbazole (**13**; R = -C_8H_{17}) with the same terminal and lateral alkyl chains. These differences can be explained by taking into account the non-coaxial and non-colinear nature of the 2,5-disubstituted thiophene bonds, with a dihedral angle of 148° between the thiophene ring and the bonds to the phenyl rings in the 2- and 5-positions, compared with the parallel and colinear bonds of the 1,4-disubstituted phenyl rings. The adoption of this dihedral angle brings the electron-rich thiophene sulphur atom and the *ortho*-hydrogen atoms on the adjacent phenyl rings close together. A dipolar attraction between these atoms should then stabilise a planar conformation of the aromatic molecular core. The *N*-octyl-2,7-bis[4'-(octyloxy)biphenyl-4-yl]carbazole (**13**; R = -C_8H_{17}) has a higher molecular length-to-breadth ratio than the *N*-octyl-2,7-*bis*-{5-[4-(octyloxy)phenyl]thiophen-2-yl}carbazole (**18**) (see Figures 4 and 3, respectively). As a consequence the nematic clearing point of *N*-octyl-2,7-bis[4'-(octyloxy)biphenyl-4-yl] carbazole (**13**; R = -C_8H_{17}) should be higher than that of *N*-octyl-2,7-*bis*-{5-[4-(octyloxy)phenyl]thiophen-2-yl}carbazole (**18**), as is indeed observed to be the case.

The *N*-octyl-2,7-bis[4'-(octyloxy)biphenyl-4-yl]carbazole (**13**; R = -C_8H_{17}), with a single octyl substituent attached to the bridging nitrogen atom of the carbazole ring, exhibits a much higher clearing point (309°C) than that (168°C) of the corresponding carbazole (**13**; R = $CH(C_8H_{17})_2$) with a branched heptadec-9-yl chain [-$CH(C_8H_{17})_2$] attached to the nitrogen atom of the central carbazole (see Table 1). This is attributable to the chain branching, which usually leads to lower transition temperatures due to steric effects. A relatively high nematic clearing point is still observed for the carbazole (**13**; R = $CH(C_8H_{17})_2$) with a branched chain, which may be attributable to both octyl chains lying in the plane of the molecule (see Figure 5). Although this idealised anti-periplanar conformation of the octyl chains in the same plane as the aromatic molecular core, which may be preferred since it allows close packing of adjacent molecules, may not lead to a significant increase of the molecular rotation volume or the intermolecular distance between adjacent molecules, it would still reduce the effective molecular length-to-breadth ratio and the resultant anisotropy of dispersion forces and the anisotropy of polarisability, leading to a lower nematic clearing point.

A comparison between the liquid crystal transition temperatures of the *N*-octyl-2,7-*bis*-{5-[4-(octyloxy)-phenyl]thiophen-2-yl}carbazole (**18**) and the analogous 2,7-disubstituted fluorene (**19**) shows that replacing the dialkyl chain in the 9-position of a 2,7-disubstituted fluorene unit with the monoalkyl chain in the same position of a 2,7-disubstituted carbazole unit has a large effect on the liquid crystalline transition temperatures and the temperature range of the nematic mesophase (see Table 1). The melting and clearing point (163°C and 228°C, respectively) of the *N*-octyl-2,7-*bis*-{5-[4-(octyloxy)phenyl]thiophen-2-yl}carbazole (**18**) are much higher than those (69°C and 99°C, respectively) of the corresponding 9,9-dioctyl-substituted fluorene (**19**) [31]. This phenomenon is clearly attributable to steric effects, which will be much smaller for the *N*-octyl-2,7-*bis*-{5-[4-(octyloxy)phenyl]thiophen-2-yl}carbazole (**18**) where the octyl chain may be forced to lie in the plane of the aromatic core of the molecule in the solid state in order to attain efficient packing (see Figure 3). The two octyl chains attached to position 9 of the fluorene (**19**) lie out of the plane of the aromatic core. In this configuration they lead to significant broadening of the molecular rotation volume, a lower length-to-breadth ratio as well as greater intermolecular separation between neighbouring molecules. A combination of these steric effects leads to weaker van der Waals forces of attraction between neighbouring molecules and the anisotropy of dispersion forces and the anisotropy of polarisability. A combination of these factors should lead to much lower liquid crystalline transition temperatures for the 9,9-dioctyl-substituted fluorene (**19**) compared with those of the related *N*-octyl-2,7-*bis*-{5-[4-(octyloxy)phenyl]thiophen-2-yl}carbazole (**18**), as is indeed observed to be the case.

3.2 Physical properties

The UV-Vis absorption and PL spectra of the *N*-octyl-2,7-*bis*-{5-[4-(octyloxy)phenyl]thiophen-2-yl}carbazole (**18**) in solution and as a thin film are shown in Figure 6. This figure shows that compound (**18**) absorbs in the ultra violet and emits light in the blue part of the spectrum. The large Stokes shift (60–80 nm) between the UV-Vis absorption and PL spectra of the carbazole (**18**) compared with that (~6–8 nm) of the corresponding bisindenocarbazoles [9, 10] is indicative of the much smaller, less rigid aromatic core of the carbazole (**18**) than that of the bisindenocarbazoles with the same number of phenyl rings in the fused aromatic core. There is a small red shift between the emission in solution (λ_{max} = 465 nm) and in the thin film (λ_{max} = 485 nm). The quantum efficiency of emission is very

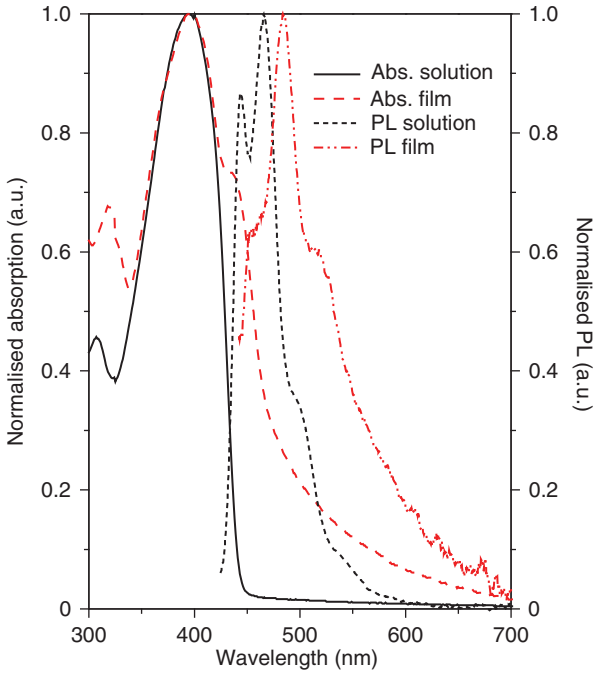

Figure 6. UV-Vis absorption and photoluminescence (PL) spectra of the 9-spiro-substituted-carbazole (**18**) in solution and as a thin solid film (colour version online).

much higher for compound (**18**) in solution (QE_{PL} = 63%) than as a thin film (QE_{PL} = 1%). The very low emission in the thin film indicates very significant quenching of the excited state. The broader tail of the UV-Vis absorption spectrum of compound (**18**) in the solid state compared with that in solution appears to confirm a substantial degree of molecular aggregation in the solid state. This suggests that the planar structure of compound (**18**) allows for close molecular packing in the solid state and short intermolecular distances. The blue PL emission (λ_{max} = 485 nm) of compound (**18**) is red-shifted with respect to that (λ_{max} = 450 nm) of the corresponding compound (**13**; R = C_8H_{17}), whose chemical structure only differs from that of compound (**18**) by having a 1,4-disubstituted phenyl ring in place of the 2,5-disubstituted thiophene ring in compound (**18**). This is attributable to a lower degree of conjugation in compound (**13**; R = C_8H_{17}) due to a higher aryl-aryl twist angle at phenyl-phenyl bonds than that at thiophene-phenyl bonds as present in compound (**18**). The PL emission (λ_{max} = 485 nm) of the carbazoles (**18**) and (**13**; R = C_8H_{17}) is considerably red-shifted compared with that (λ_{max} = ~400 nm) of the related bisindenocarbazoles [9, 10].

The data collated in Table 2 reveal significant differences in the values for the IP, EA and E_g of the carbazole (**13**; R = $CH(C_7H_{15})_2$) and the related 9,9-dibutyl-substituted fluorene (**20**) where a 2,7-disubstituted fluorene moiety has replaced the 2,7-disubstituted carbazole group. The aliphatic substituents are not identical for the carbazole (**13**; R = $CH(C_7H_{15})_2$) and the fluorene (**20**). However, we have shown that the nature of the aliphatic substituents in the 9-position (cyclic or linear) and aliphatic terminal chains (alkoxy-chain or alkoxy-chain plus polymerisable diene or oxetane endgroup) have very limited effects on the IP and EA of very similar compounds [36], and so the comparison may still be regarded as informative. The replacement of the fluorene moiety by the carbazole group reduces the absorption edge wavelength and reduces the optical energy band gap $E_{g,op}$ as shown in Figure 7(a). The oxidation potential onset is lower, as shown in Figure 7(b), and so the IP is reduced. Therefore, the presence of the nitrogen atom in the carbazole (**13**; R = $CH(C_7H_{15})_2$) increases the Highest Occupied Molecular Orbit level and reduces the Lowest Unoccupied Molecular Orbit level compared with the related 9,9-dipropyl-substituted fluorene (**20**), as shown in Figure 8; i.e. the band gap (2.9 eV) of the carbazole (**13**; R = $CH(C_7H_{15})_2$) is smaller than that (3.1 eV) of the fluorene (**20**). The lower IP (5.55 eV) of the carbazole (**13**; R = $CH(C_7H_{15})_2$) than that (5.86 eV) of the fluorene (**20**) suggests that such carbazoles may have the potential be good hole transport materials in OLEDs or as electron donors in organic photovoltaics. However, the irreversible cyclic voltagram indicates insufficient electrochemical stability for practical applications, such as in OLEDs, although this should be tested in prototype devices to confirm this conclusion. TGA of the carbazole (**18**) and the reference 9,9-dialkyl fluorenes (**19**), differing only in the bridging central group, reveals that the onset of degradation (equating to 5% mass loss) occurs at a higher temperature (398°C) for the carbazole (**18**) than that (381°C equating to 5% mass loss) of the corresponding 9,9-dialkyl fluorene (**19**). These data indicate that the carbazole (**18**) is marginally more thermally stable than the corresponding 9,9-dialkyl fluorene (**19**).

Table 2. The ionisation potential (IP), electron affinity (EA) and the band gap (E_g) of the carbazole (**13**; R = -$CH(C_7H_{15})_2$) and the 9,9-dibutyl-substituted fluorene (**20**).

	IP[a] eV	E_g[b] eV	EA[c] eV	Remark
(**13**; R = -$CH(C_7H_{15})_2$)	5.78	2.92	2.86	irreversible
(**20**)	5.86	3.1	2.76	irreversible

Notes: [a]Determined by CV; [b]obtained from optical absorption spectrum; [c]calculated from IP – E_g.

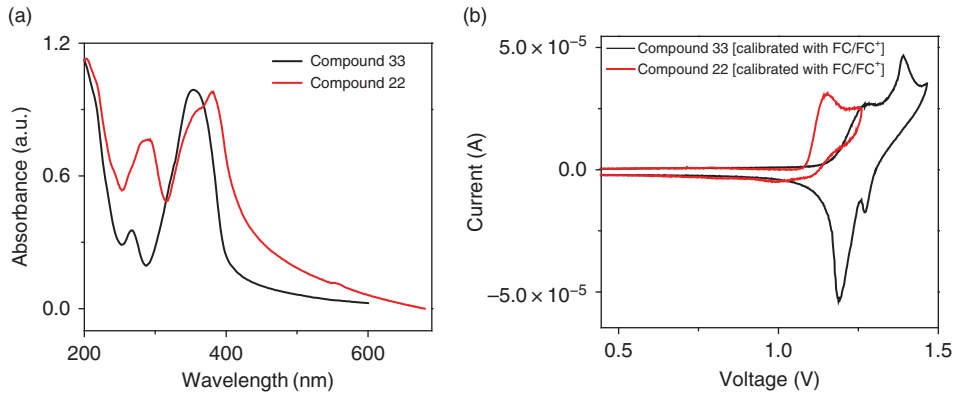

Figure 7. (a) Normalised absorption spectrum of the carbazole (**13**; R = $CH(C_7H_{15})_2$) and the related 9,9-dipropyl-substituted fluorene (**20**). (b) Cyclic voltammogram onset of the same compounds (calibrated with Fc/Fc^+) (colour version online).

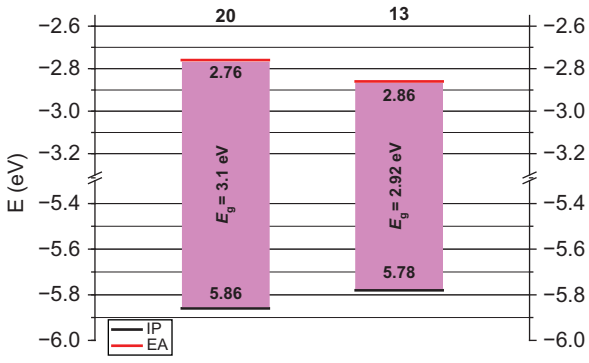

Figure 8. HOMO/LUMO energy levels of the carbazole (**13; R = $CH(C_7H_{15})_2$**) and the related 9,9-dibuyl-substituted fluorene (**20**) (colour version online).

4. Conclusions

A small number of 2,7-diaryl-*N*-alkyl-substituted carbazole derivatives with a nematic phase have been synthesised for the first time as model compounds. Branching of the aliphatic chain attached to the bridging nitrogen atom in the carbazole ring leads to a significantly lower nematic temperature range compared with that of a straight-chain analogue. Molecular modelling suggests that the *N*-alkyl chain lies primarily in the plane of the aromatic core of the molecule, which allows short intermolecular distances, which may be responsible for the high melting points observed. The UV-Vis absorption spectra and the low quantum efficiency PL emission of thin films of these materials are consistent with this interpretation. The relatively low IP of the carbazole (**13**; R = $CH(C_7H_{15})_2$) implies that they may be good potential hole transport materials or as electron donors in OPV. Unfortunately, the irreversible cyclic voltagram indicates insufficient electrochemical stability for practical electro-optical or electronic applications.

Acknowledgements

We thank the EPSRC for the award of a postdoctoral fellowship to Dr S.P. Kitney and visiting studentship support for Dr Pan Wei, the University of Hull and the China Scholarship Council for a studentship to Weixiao Bao, the Saudi Arabian Government for the award of a PhD studentship to Mr M.S. Al-Kalifah and the Spanish Government for a postdoctoral fellowship to Dr M. Haro. We express our thanks to Dr R. Lewis (^{1}H NMR) and Dr K. Welham (MS) for spectroscopic measurements and Mrs K. Kennedy for combustion analyses.

References

[1] Funahashi, M.; Hanna, J.I. *Jpn. J. Appl. Phys*. **1996**, *35*, L703–L706.
[2] Funahashi, M.; Hanna, J.I. *Phys. Rev. Lett*. **1997**, *78*, 2184–2187.
[3] Bacher, A.; Bently, P.G.; Bradley, D.D.C.; Douglas, L.K.; Glarvey, P.A.; Grell, M.; Whitehead, K.S.; Turner, M.L. *J. Mater. Chem*. **1999**, *9*, 2985–2989.
[4] O'Neill, M.; Kelly, S.M. *Adv. Mater. (Weinheim, Ger.)* **2003**, *15*, 1135–1146.
[5] Kreouzis, T.; Baldwin, R.J.; Shkunov, M.; McCulloch, I.; Heeny, M.; Zhang, W. *Appl. Phys. Lett*. **2005**, *87*, 172110–1–3.
[6] McCulloch, I.; Heeney, M.; Bailey, C.; Genevicius, K.; Macdonald, I.; Shkunov, M.; Sparrowe, D.; Tierny, S.; Wagner, R.; Zhang, W.; Chabinyc, M.L.; Kline, R.J.; McGehee, M.D.; Toney, M.F. *Nature (London, UK)* **2006**, *5*, 328–333.
[7] Baldwin, R.J.; Kreouzis, T.; Shkunov, M.; Heeny, M.; Zhang, W.; McCulloch, I. *J. Appl. Phys*. **2007**, *101*, 023713–1–10.
[8] Shimizu, Y.; Oikawa, K.; Nakayama, K.-I.; Guillon, D. *J. Mater. Chem*. **2007**, *17*, 4223–4229.
[9] Sonntag, M.; Strohriegl, P. *Tetrahedron Lett*. **2006**, *47*, 8313–8108.
[10] Sonntag, M.; Strohriegl, P. *Liq. Cryst*. **2007**, *34*, 49–57.
[11] Sonntag, M.; Strohriegl, P. *Tetrahedron* **2006**, *62*, 8103–8317.
[12] Sienkowska, M.J.; Monobe, H.; Kaszynski, P.; Shimizu, Y. *J. Mater. Chem*. **2007**, *17*, 1392–1398.

[13] Donvan, K.J.; Scott, K.; Somerton, M.; Preece, J.; Manickam, M. *Chem. Phys*. **2006**, *322*, 471–476.
[14] Perea, E.; Lopez-Calahorra, F.; Velasco, D. *Liq Cryst*. **2002**, *29*, 421–428.
[15] Manickam, M.; Kumar, S.; Preece, J.A.; Spencer, N. *Liq. Cryst*. **2000**, *27*, 703–706.
[16] Manickam, M.; Belloni, M.; Kumar, S.; Varshney, S.K.; Shankar Roa, D.S.; Ashton, P.R.; Spencer, N. *J. Mater. Chem*. **2001**, *11*, 2790–2800.
[17] Kosaka, Y.; Kato, T.; Uryu, T. *Macromolecules* **1994**, *27*, 2658–2663.
[18] Kosaka, Y.; Uryu, T. *Macromolecules* **1995**, *28*, 870–875.
[19] Lux, M.; Strohriegl, P.; Höcker, H. *Makromolekulare Chem*. **1986**, *188*, 811–820.
[20] Arnim, V.V.; Finkelmann, H.; Dobarro, A.; Velasco, D. *Macromol. Chem. Phys*. **1996**, *197*, 2729–2743.
[21] Dobarro, A.; Velasco, D.; Arnim, V.V.; Finkelmann, H. *Macromol. Chem. Phys*. **1997**, *198*, 2563–2581.
[22] Blouin, N.; Michaud, A.; Leclerc, M. *Adv. Mater. (Weinheim, Ger.)* **2007**, *19*, 2295–2300.
[23] Bouchard, J.; Wakim, S.; Leclerc, M. *J. Org. Chem*. **2004**, *69*, 5705–5711.
[24] Yoshida, Y.; Sakakura, Y.; Aso, N.; Okada, S.; Tanabe, Y. *Tetrahedron* **1999**, *55*, 2183–2192.
[25] Dierschke, F.; Grimsdale, A.C.; Müllen, K. *Synthesis* **2003**, *16*, 2470–2472.
[26] Mazoni, G.; Garbrecht, W.L. *Synthesis* **1987**, 651–653.
[27] Aldred, M.P.; Eastwood, A.J.; Kelly, S.M.; Vlachos, P.; Contoret, A.E.A.; Farrar, S.R.; Mansoor, B.; O'Neill, M.; Tsoi, W.-C. *Chem. Mater*. **2004**, *16*, 4928–4936.
[28] Williamson, A. *Justus Liebigs Ann. Chem*. **1851**, *77*, 37.
[29] Miyaura, N.; Yangai, T.; Suzuki, A. *Synth. Commun*. **1981**, *11*, 513–519.
[30] Grosu, I.; Ple, G.; Mager, S.; Mesaros, E.; Dulau, A.; Gego, C. *Tetrahedron* **1998**, *54*, 2905–2916.
[31] Aldred, M.P.; Eastwood, A.J.; Kitney, S.P.; Richards, G.J.; Vlachos, P.; Kelly, S.M.; O'Neill, M. *Liq. Cryst*. **2005**, *32*, 1251–1264.
[32] Miller, L.L.; Yu, Y. *J. Org. Chem*. **1995**, *60*, 6813–6819.
[33] Stille, J.K. *Angew. Chem. Int. Ed. Engl*. **1986**, *25*, 508–524.
[34] de Mello, J.C.; Wittmann, H.F.; Friend, R.H. *Adv. Mater. (Weinheim, Ger.)* **1997**, *9*, 230–232.
[35] Bredas, J.L.; Silbey, R.; Boudreaux, D.S.; Chance, R.R. *J. Am. Chem. Soc*. **1983**, *105*, 6555–6559.
[36] Kassireddy, K.; Billa, M.R.; Haro, M.; Al-Kalifah, M.S.; Kelly, S.M.; Kitney, S.P.; O'Neill, M. *Liq. Cryst*. to be submitted.